

Thiago Antonini Alves

thiagoalves@utfpr.edu.br
 Universidade Tecnológica Federal do Paraná
 Engenharia Mecânica
 84016-210 Ponta Grossa, PR, Brasil

Carlos A. C. Altemani

altemani@fem.unicamp.br
 Universidade Estadual de Campinas
 Faculdade de Engenharia Mecânica
 Departamento de Energia
 13083-970 Campinas, SP, Brazil

Conjugate Cooling of a Discrete Heater in Laminar Channel Flow

Electronic components are usually assembled on printed circuit boards cooled by forced airflow. When the spacing between the boards is small, there is no room to employ a heat sink on critical components. Under these conditions, the components' thermal control may depend on the conductive path from the heater to the board in addition to the direct convective heat transfer to the airflow. The conjugate forced convection-conduction heat transfer from a two-dimensional strip heater flush mounted to a finite thickness wall of a parallel plates channel cooled by a laminar airflow was investigated numerically. A uniform heat flux was generated along the strip heater surface. Under steady state conditions, a fraction of the heat generation was transferred by direct convection to the airflow in the channel and the remaining fraction was transferred by conduction to the channel wall. The lower surface of the channel wall was adiabatic, so that the heat conducted from the heater to the plate eventually returned to the airflow. A portion of it returned upstream of the heater, preheating the airflow before it reached the heater surface. Due to this, it was convenient to treat the direct convection from the heater surface to the airflow by the adiabatic heat transfer coefficient. The flow was developed from the channel entrance, with constant properties. The conjugate problem was solved numerically within a single solution domain comprising both the airflow region and the solid wall of the channel. The results were obtained for the channel flow Reynolds number ranging from about 600 to 1900, corresponding to average airflow velocities from 0.5 m/s to 1.5 m/s. The effects of the solid wall to air thermal conductivities ratio were investigated in the range from 10 to 80, typical of circuit board materials. The wall thickness influence was verified from 1 mm to 5 mm. The results indicated that within these ranges, the conductive substrate wall provided a substantial enhancement of the heat transfer from the heater, accomplished by an increase of its average adiabatic surface temperature.

Keywords: conjugate heat transfer, adiabatic heat transfer coefficient, laminar channel flow, numerical analysis

Introduction

The purpose of the present work was to perform an analysis of the conjugate forced convection-conduction heat transfer from a small 2D foil heater flush mounted to the lower plate (substrate) of a horizontal channel, as indicated in Fig. 1. The substrate thickness (t) and its thermal conductivity (k_s) were known and a laminar developed airflow was forced into the channel. The lower surface and both ends of the substrate plate were adiabatic, so that only the upper face, in contact with the airflow, could exchange heat by forced convection. There were two thermal paths available for heat transfer from the heater to the airflow. One was by convection, directly from the heater upper surface to the airflow. The other was from the heater lower surface by conduction and spreading in the substrate wall. The heat transfer through this path was transferred back to the airflow by convection at the upper substrate surface, both upstream and downstream of the heater. This substrate conduction presents two opposing effects to the heater cooling by the airflow. First, a thermal boundary layer development upstream the heater reduces the direct convective heat transfer from the heater to the airflow. On the other hand, the effective heat transfer area to the airflow increases due to the conductive spreading upstream and downstream the heater. If this effect prevails over the first one, there will be a heat transfer enhancement, as compared to the case of an adiabatic substrate plate.

The effects of the laminar airflow rate, the fluid to substrate thermal conductivities ratio and the substrate thickness were considered in the present analysis. The total heat dissipation rate in the heater was assumed known, but its distribution into the direct convection to the airflow and the conduction to the substrate wall was obtained from analysis. The convective heat transfer was characterized by the adiabatic heat transfer coefficient h_{ad} , due to its independence on the thermal boundary conditions (Moffat, 1998; Alves and Altemani, 2008). The heat transfer coefficient based on the inlet flow temperature (T_{in}) was also evaluated for comparison

with the adiabatic coefficient. This problem depends also on the heater length and position in the channel. In the present work, the heater length was equal to the channel height and its upstream edge was centered on the substrate.

A comprehensive review of the work on conjugate forced convection-conduction heat transfer from electronic components was presented by Nakayama (1997), considering distinct heat source geometries and their arrangement on the wiring board. Here, the emphasis will be directed to works associated to flush mounted heat sources. Ramadhyani et al. (1985) presented results of a 2D numerical analysis of the conjugate heat transfer from two discrete heat sources flush mounted on one wall of a channel. The heaters were isothermal and the wall on which they were flush mounted was a thick conductive substrate. The coolant flow was laminar and fully developed, and the analysis encompassed a range of the wall to fluid thermal conductivities ratio. The reference temperature for the Nusselt number was the inlet flow temperature. Their results indicated that the fraction of heat transfer from the heat source to the substrate can be a major contribution to the total heat transfer – it increased with the substrate to fluid thermal conductivity ratio and for low fluid Peclet numbers. Incropera et al. (1986) performed experiments and numerical analysis of the problem of flush mounted isothermal heat sources on a thick insulated wall of a horizontal channel. The flow was fully developed either in the laminar or the turbulent regime. The reference temperature for the Nusselt number was the fluid inlet temperature in the channel. The calculation domain for the numerical analysis of the conjugate problem involved the solid and fluid regions. Their numerical model predictions were in good agreement with measurements for turbulent flow, but for laminar flow the predictions were lower than the measurements. Anderson (1994) presented a technique to decouple the conjugate conductive and convective heat transfer from electronic modules on a circuit board. The adiabatic heat transfer coefficient (an invariant descriptor of the local convective heat transfer) was used with a superposition method to interface between a convection solver and a conductor solver. The method was recommended for the cooling of a module on a circuit board

Paper received 2 February 2011. Paper accepted 23 May 2011.
 Technical Editor: Horácio Vielmo.

whenever a Biot number based on the ratio of the module's resistance to conduction over that to convection was greater than 1. Sugavanam et al. (1995) presented a numerical analysis of the conjugate heat transfer from 2D uniformly powered strip heaters flush mounted on the lower wall of a horizontal parallel plates channel. The substrate wall upper surface was cooled by laminar forced convection and the lower surface was either adiabatic or subject to laminar forced convection. The dependence of the heat transfer from the heat source was investigated for a wide range of parameters, including the substrate to coolant fluid thermal conductivities ratio (k_s/k), the heat source position and the channel Reynolds number. The results indicated that preheating of the flow by board conduction increased with the ratio (k_s/k), decreasing the Nusselt number on the heat source. The reference temperature for the Nusselt number was the fluid inlet temperature. It was verified that the effects of substrate thickness were important only for the conductivity ratio (k_s/k) > 10. The average Nusselt on the heater surface decreased with an increase in (k_s/k) for fully developed flow, due solely to substrate conduction effects. This decrease was more pronounced for smaller values of the Reynolds number, due to the relative increase of the substrate conduction effect. Considering a uniform flow at the channel entrance, developing along the channel length, the average Nusselt on the heater surface decreased as the source moved to downstream positions in the channel. Cole (1997) presented an analysis for the conjugate convective-conductive heat transfer from a 2D strip heater flush mounted on the surface of a conductive plate of finite thickness. The plate was cooled on the heater side by a fluid flow with a linear velocity profile, while the opposite surface was adiabatic. The reference temperature for the Nusselt number was that of the coolant fluid far from the plate surface, typical for external flows. The heat transfer numerical results were presented in terms of a conjugate Peclet number. It was found that for large values of this parameter, the heat transfer is dominated by the fluid flow and the strip heater size is the appropriate length scale. For small values, the appropriate scale was the solid thickness. Wang and Jaluria (2004) considered the effects of the three-dimensional conjugate mixed convection and conduction heat transfer from two heaters flush mounted on the lower wall of a horizontal rectangular duct. The two heaters were deployed with both streamwise and spanwise separation on the wall. The effects of the wall to fluid thermal conductivities ratio and the Reynolds number in the laminar regime, considering a single value of the Grashoff number, were presented in the numerical results. Among their conclusions, the heaters spanwise distribution may result in lower average temperature for the two sources. Considering a duct with an aspect ratio of 10, they reported that the numerical results of temperature distribution on the solid-fluid interface were slightly lower than those of Sugavanam et al. (1995). This was attributed to conduction in the spanwise direction, associated to the three-dimensional simulations.

In the present investigation, a numerical solution of the conjugate problem was performed for a single domain comprising both the solid and fluid regions. The reference temperature selected to describe convective heat transfer from the heater was its average adiabatic surface temperature. Thus, the corresponding average adiabatic heat transfer coefficient is independent of the amount of airflow preheating upstream of the heater. This preheating is due to the thermal wake generated by conduction upstream of the heater through the substrate plate.

Natural convection effects were considered negligible in the present work, a procedure adopted in similar investigations (e.g., Alves and Altemani, 2010; Zeng and Vafai, 2009; Davalath and Bayazitoglu, 1987 and Ramadhyani et al., 1985). In order to present a perspective for this consideration, reference will be made to the work of Kang et al. (1990). They performed experiments to

investigate the mixed convection from a single heat source module mounted on a thin horizontal plate well insulated at the back surface. Their results indicated that the heat transfer from the module is dominated by forced convection when $(Gr/Re^{5/2}) < 0.9$. The Reynolds number Re was based on the heater length and the forced flow average velocity. The Grashoff number was $Gr = g\beta q''(L+2H)L^3/(k v^2)$, where L and H indicate respectively the heater length and height, and q'' is the convective heat flux from the module to the fluid. When the heater is flush mounted on the substrate plate, the height is $H = 0$. For any specified value of Re , their correlation gives the upper limit of Gr for which natural convection effects may be neglected.

The results of the present investigation are important for the thermal design of electronic components assembled on circuit boards cooled by forced convection. The conjugate forced convection and conduction heat transfer must be accounted for, and this analysis is most important under conditions of limited available spacing between the boards. In this case, heat sinks may not be allowed for cooling purposes and the heat transfer enhancement due to heat spreading along the substrate wall may be an important contribution to the total heat transfer (Alves, 2010).

Nomenclature

c_p	= specific heat, J/(kg.K)
g^*	= influence coefficient
h	= convective heat transfer coefficient, W/(m ² .K)
H	= channel height, m
k	= air thermal conductivity, W/(m.K)
k_s	= substrate thermal conductivity, W/(m.K)
L	= total channel length, m
L_d	= downstream length, m
L_h	= heater length, m
L_u	= upstream length, m
\dot{m}	= mass flow rate, kg/s
Nu	= Nusselt number
Pe	= Peclet number
Pr	= Prandtl number
q	= convective heat transfer rate per unit heater depth, W/m
q''	= heat flux, W/m ²
Re	= Reynolds number, Eq. (2)
t	= substrate thickness, m
T	= temperature, K
u	= velocity component along the plates, m/s
U	= dimensionless u – velocity component, Eq. (6)
x, y	= Cartesian coordinates, m
X, Y	= dimensionless Cartesian coordinates, Eq. (6)

Greek Symbols

ρ	= density, kg/m ³
μ	= dynamic viscosity, Pa.s
θ	= dimensionless temperature, Eq. (6)
ζ	= dimensionless coordinates

Subscripts

ad	= adiabatic
d	= downstream
f	= fluid
h	= heater
in	= inlet
m	= mixed mean
s	= substrate
u	= upstream

Superscripts

–	= average
---	-----------

Analysis

Problem formulation and heat transfer parameters

A small foil heater (length L_h) is flush mounted on a conductive substrate with thickness t and thermal conductivity k_s in a horizontal channel of length L and height H , as indicated in Fig. 1. The substrate lower and side surfaces, as well as the channel upper surface, are all adiabatic.

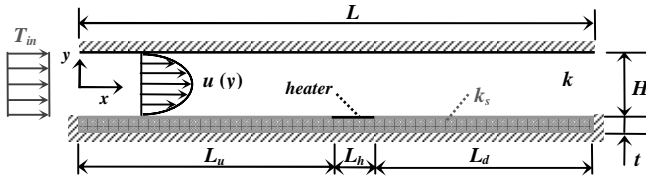


Figure 1. Schematic of the conjugate heat transfer problem.

A laminar airflow, with constant properties evaluated at 300 K, was developed from the channel entrance, with uniform velocity \bar{u} and the analytical parabolic velocity profile given by

$$u(y) = \frac{3}{2}\bar{u}\left(1 - \frac{4y^2}{H^2}\right), \quad -\frac{H}{2} \leq y \leq \frac{H}{2} \quad (1)$$

The average airflow velocity \bar{u} and the channel hydraulic diameter defined the Reynolds number

$$Re = \frac{\rho\bar{u}2H}{\mu} \quad (2)$$

The heater upstream edge was positioned at $L_u = L/2$ on the upper substrate surface. A heat dissipation rate equal to q_h per unit depth normal to Fig. 1 was uniformly distributed along the heater length, with a heat flux $q_h'' = q_h/L_h$. This heat flux was distributed either directly to the airflow above the heater, with local flux $q_f''(x)$, or to the substrate under the heater, with a local flux $q_s''(x)$. Under steady state conditions, a local energy balance along the heater requires that

$$q_h'' = q_f''(x) + q_s''(x) \quad (3)$$

The local heat fluxes $q_f''(x)$ and $q_s''(x)$ were obtained by an iterative numerical solution of the energy equation in the conjugate domain indicated in Fig. 1, comprising the solid substrate, the heater and the flow regions. In dimensionless form, the energy conservation equations respectively for the solid and fluid regions were expressed as follows:

$$\frac{1}{Pr} \frac{k_s}{k} \left(\frac{\partial^2 \theta}{\partial X^2} + \frac{\partial^2 \theta}{\partial Y^2} \right) = 0, \quad 0 \leq X \leq 1, \quad -\left(\frac{H}{2L} + \frac{t}{L}\right) \leq Y \leq -\frac{H}{2L} \quad (4)$$

$$U \frac{\partial \theta}{\partial X} = \frac{1}{Pr} \left(\frac{\partial^2 \theta}{\partial X^2} + \frac{\partial^2 \theta}{\partial Y^2} \right), \quad 0 \leq X \leq 1, \quad -\frac{H}{2L} \leq Y \leq \frac{H}{2L} \quad (5)$$

The dimensionless variables were

$$X = \frac{x}{L}, \quad Y = \frac{y}{L}, \quad U = \frac{\rho u L}{\mu}, \quad \theta = \frac{k(T - T_{in})}{q_h'' L_h} \quad (6)$$

Equations (4) and (5) were solved simultaneously, subject to the following boundary conditions. The upper and lower surfaces of the domain, as well as the upstream and downstream ends of the substrate plate were adiabatic. At the channel inlet, the fluid temperature was uniform at T_{in} , which corresponds to $\theta_{in} = 0$. The outflow boundary was treated with negligible diffusion. At the substrate-fluid interface, the temperature and heat flux continuity were imposed as follows.

$$\theta|_s = \theta|_f, \quad 0 \leq X \leq 1, \quad Y = -\frac{H}{2L} \quad (7)$$

$$\frac{k_s}{k} \frac{\partial \theta}{\partial Y}|_s = \frac{\partial \theta}{\partial Y}|_f, \quad X < \frac{L_u}{L} \quad \text{and} \quad X > \left(1 - \frac{L_d}{L}\right), \quad Y = -\frac{H}{2L} \quad (8)$$

$$\frac{k_s}{k} \frac{\partial \theta}{\partial Y}|_s - \frac{\partial \theta}{\partial Y}|_f = \frac{L}{L_h}, \quad \frac{L_u}{L} \leq X \leq \left(1 - \frac{L_d}{L}\right), \quad Y = -\frac{H}{2L} \quad (9)$$

Equation (9) is the dimensionless form of the local energy balance expressed by Eq. (3). The heater surface temperature $T_h(x)$ and the heat fluxes $q_f''(x)$ and $q_s''(x)$ were not uniform along the heater length L_h . They were integrated along the heater length to obtain, respectively, the average heater temperature and the heat transfer rates q_f from the heater directly to the airflow and q_s to the solid substrate.

$$\bar{T}_h = \frac{1}{L_h} \int_{L_h} T_h(x) dx, \quad q_f = \int_{L_h} q_f''(x) dx, \quad q_s = \int_{L_h} q_s''(x) dx \quad (10)$$

Obviously, the local energy balance expressed by Eq. (3), after integration over the heater length, results in the overall energy balance $q_h = q_f + q_s$.

Two average convective heat transfer coefficients were defined on the heater surface. One was \bar{h}_{ad} , based on the heater average adiabatic surface temperature, \bar{T}_{ad} . This coefficient is important because it is independent of the thermal conditions upstream the heater (Alves and Altemani, 2008). The heater adiabatic surface temperature may be obtained mostly, simply considering an adiabatic substrate wall, because in this case it is equal to the airflow inlet temperature. In this case, all dissipated heat is transferred directly to the airflow ($q_f = q_h$), so that

$$\bar{h}_{ad} = \frac{q_h}{L_h (\bar{T}_{ad} - T_{in})} \Big|_{k_s=0} \quad (11)$$

The average adiabatic Nusselt number over the heater was expressed by

$$\overline{Nu}_{ad} = \frac{\bar{h}_{ad} L_h}{k} = \frac{1}{\theta_h} \Big|_{k_s=0} \quad (12)$$

The other average heat transfer coefficient was \bar{h}_{in} , based on the uniform inlet flow temperature T_{in} . It was obtained considering a conductive substrate ($k_s \neq 0$), for which a fraction (q_f/q_h) of the total dissipation rate q_h was transferred directly to the airflow, defined by:

$$\bar{h}_{in} = \frac{q_f}{L_h(\bar{T}_h - T_{in})} \quad (13)$$

The corresponding average Nusselt number in this case was

$$\overline{Nu}_{in} = \frac{\bar{h}_{in} L_h}{k} = \frac{q_f}{q_h} \frac{1}{\bar{\theta}_h} \quad (14)$$

For a conductive substrate, the heater average temperature rise above the inlet flow temperature ($\bar{T}_h - T_{in}$) is due to two effects. The direct convective heat transfer rate q_f from the heater to the airflow is responsible for the heater temperature rise above its adiabatic temperature, ($\bar{T}_h - \bar{T}_{ad}$). The heat transfer rate q_u conducted through the substrate wall upstream the heater returns by convection to the airflow. This effect gives rise to a thermal wake responsible for the heater adiabatic temperature rise above the inlet flow temperature, ($\bar{T}_{ad} - T_{in}$). These two effects may be added as follows:

$$(\bar{T}_h - T_{in}) = (\bar{T}_h - \bar{T}_{ad}) + (\bar{T}_{ad} - T_{in}) \quad (15)$$

Due to imperfect fluid mixing in the channel, the adiabatic temperature rise ($\bar{T}_{ad} - T_{in}$) is always greater than the corresponding fluid mixed mean temperature rise ($T_{m,u} - T_{in}$). The ratio of these two temperature differences defined a coefficient g_u^* . An energy balance in the flow region upstream the heater related ($T_{m,u} - T_{in}$) to q_u and the airflow rate \dot{m} .

$$(\bar{T}_{ad} - T_{in}) = (T_{m,u} - T_{in}) g_u^* = \frac{q_u}{\dot{m} c_p} g_u^* \quad (16)$$

Similarly, the heater average temperature rise ($\bar{T}_h - \bar{T}_{ad}$) was related, by an influence coefficient g_h^* , to the corresponding fluid mixed mean temperature rise $(\Delta T_m)_h$, which was expressed in terms of q_f and the flow rate \dot{m} .

$$(\bar{T}_h - \bar{T}_{ad}) = (\Delta T_m)_h g_h^* = \frac{q_f}{\dot{m} c_p} g_h^* \quad (17)$$

Substituting Eqs. (16) and (17) into Eq. (15),

$$(\bar{T}_h - T_{in}) = \frac{q_f}{\dot{m} c_p} g_h^* + \frac{q_u}{\dot{m} c_p} g_u^* \quad (18)$$

Defining the Peclet number $Pe = RePr$, Eq. (18) was obtained in dimensionless form.

$$\bar{\theta}_h = \frac{2}{Pe} \left(\frac{q_f}{q_h} g_h^* + \frac{q_u}{q_h} g_u^* \right) \quad (19)$$

The fractions (q_f/q_h) and (q_u/q_h) and the upstream coefficient g_u^* depend on the conduction through the substrate and were obtained for each test condition. The convective coefficient g_h^* , on the other hand, depends solely on the flow conditions and it was obtained from numerical tests considering an adiabatic substrate wall.

Problem formulation and heat transfer parameters

The energy equations (4) and (5) were solved simultaneously within the conjugate domain indicated in Fig. 1, comprising the solid substrate and the flow regions, using the control volumes method (Patankar, 1980). The convection and diffusion in the flow region, described by Eq. (5), with fully developed flow in the channel, were treated by the power-law scheme. The linear system of algebraic equations obtained from the discretization process was solved iteratively using the line-by-line TDMA method. The numerical results were obtained imposing the stated boundary conditions and the temperature and heat flux continuity expressed by Eqs. (7) to (9) along the substrate-fluid interface. Equations (7) and (8) were automatically satisfied by the use of the harmonic mean for evaluation of the diffusion coefficients at the control volumes interfaces. Equation (9) indicates the distribution of the uniform heat flux q_h'' into the local heat fluxes $q_f''(x)$ and $q_s''(x)$ and required an iterative solution procedure, described as follows. Along the heater length, the link between the adjacent solid and fluid control volumes, respectively below and above the heater, was removed. An initial guess of the heat fluxes $q_f''(x)$ and $q_s''(x)$ was assumed and used to apply source terms to the referred solid and fluid control volumes. Then, the energy equations (4) and (5) were solved and the numerically obtained temperature distributions, together with Eq. (9), were used to evaluate a new heater temperature distribution $T_h(x)$ on the solid substrate-fluid interface. In the present work, a perfect thermal contact was assumed between the heater and the substrate. From the evaluated $T_h(x)$, new distributions for $q_f''(x)$ and $q_s''(x)$ were obtained and the process was repeated until convergence. Then, the upstream heating rate q_u was obtained from the substrate temperature distribution and Eq. (19) was employed to determine the coefficient g_u^* .

The results were obtained with a non-uniform two-dimensional numerical grid deployed on the solution domain, comprising 300 control volumes in the flow direction and 24 to 40 control volumes in the transversal direction. In the flow direction, the grid was most refined over the heater, which contained 80 uniformly distributed control volumes. Along the upstream length L_u , 170 control volumes were uniformly deployed, and 50 others were distributed along the downstream length L_d . Along the y -direction, the grid consisted of 20 non-uniform control volumes along the height H and 4 control volumes uniformly distributed along each mm of the substrate thickness t . In the flow region, the grid size was finer near the upper and lower solid surfaces and increased with a geometric progression toward the center of the channel.

Several grids were tested before the final distribution was selected to obtain the numerical results. The initial numerical grid tests were performed under the conditions of $Re = 1260$ and an adiabatic substrate. The number of grid points uniformly distributed along the upstream and downstream lengths was increased until 170 points along L_u and 50 points along L_d indicated that further grid refinement would not change the results. Uniform grids were tested along the heater length L_h employing 10 to 100 grid points in the x -direction, while in the fluid region uniform grids were tested from 10 to 80 grid points in the y -direction. The Richardson extrapolation technique (De Vahl Davis, 1983) was employed and indicated that the increase of the numerical error with the grid spacing was quadratic. The exact extrapolated values of the average Nusselt number over the heater were within 0.10% of the results obtained with a uniform grid of 80 x 80 grid points over the heater. Additional tests were performed employing non-uniform grids along the y -direction in the fluid region, with a geometric progression increase of the grid spacing from the top and bottom boundary surfaces of the domain. In this case, for the same uniform grid with

80 points along the heater and a non-uniform grid with only 20 points in the y -direction, the average Nusselt number was within 0.05% of the value previously obtained by extrapolation. When a conductive substrate was considered, additional tests verified that 4 grid points per mm along the y -direction in the solid region were enough to obtain results independent of further grid refinement. The grid used to obtain the results for a substrate thickness $t/H = 0.5$ is presented in Fig. 2. It is non-uniform and contains 300 control volumes along the flow and 40 control volumes in the transversal direction.

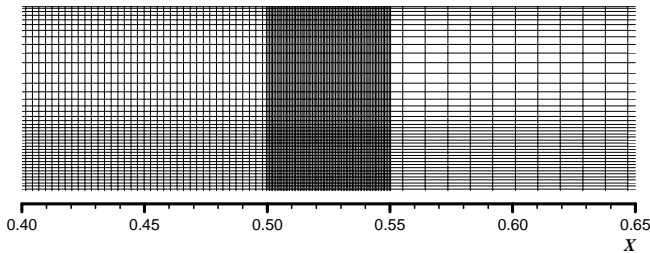


Figure 2. Non-uniform grid for $t/H = 0.5$, with (300 x 40) control volumes.

The iterative solution process was interrupted when the absolute changes of the heater average temperature $\bar{\theta}_h$, the average Nusselt number \bar{Nu}_{in} , and the heat flow ratio (q_s/q_h) between two consecutive iterations were smaller than 10^{-5} . The numerical results were obtained in a microcomputer (Intel® Pentium® D processor 2.8 GHz and 1GB RAM), in about 10 minutes for a typical solution considering a conductive substrate.

Results

The numerical results were obtained considering a channel length $L = 0.2$ m and the plates spacing $H = 0.01$ m. The heater length was $L_h = 0.01$ m, with its upstream edge at $L_u = 0.1$ m from the channel entrance. Five values were considered for the substrate thickness t , from 1 to 5mm. The effect of the substrate conductivity was investigated for five values of (k_s/k) in the range from 10 to 80. The flow was always in the laminar regime and five values of the Reynolds number were considered, in the range from about 600 to 1900 (average air velocities from 0.5 m/s to 1.5 m/s). The air properties were obtained from tabulated values at 300 K (Incropera et al., 2006).

Shah and London (1978) presented a laminar flow correlation for the local Nusselt number along a parallel plates channel with uniform heat flux on the walls, defined as follows.

$$Nu(\xi) = \frac{q''(\xi)}{T_h(\xi) - T_m(\xi)} \frac{2H}{k} \tag{20}$$

It is based on a dimensionless coordinate ξ with origin at the heater upstream length, $\xi = (x - L_u) / (2H RePr)$, on the local mixed mean airflow temperature $T_m(\xi)$ and on the channel hydraulic diameter. Their correlation is given by

$$Nu(\xi) = 1.490 \xi^{-1/3}, \quad \xi \leq 0.0002 \tag{21}$$

$$Nu(\xi) = 1.490 \xi^{-1/3} - 0.4, \quad 0.0002 \leq \xi \leq 0.001 \tag{22}$$

This correlation can be associated with that along the heater on the adiabatic substrate in the present work. A local Nusselt number $Nu_{ad}(\xi)$ based on the adiabatic heater temperature (which is equal to T_{in} when $k_s = 0$), and on the heater length, can be related to that defined in Eq. (20) by

$$Nu(\xi) = Nu_{ad}(\xi) \left[\frac{T_h(\xi) - T_{in}}{T_h(\xi) - T_m(\xi)} \frac{2H}{L_h} \right] \tag{23}$$

After substituting the correlation Eq. (21) or (22) on the left side of this equation, the resulting $Nu_{ad}(\xi)$ from the right side was compared with the numerical distribution obtained in the present work for a particular value of Re . The results obtained for $Re = 1890$ are shown in Fig. 3. They indicated that the predictions from Eq. (21) were 0.5% above the present numerical results, while Eq. (22) predicted values 1.4% below the numerical values.

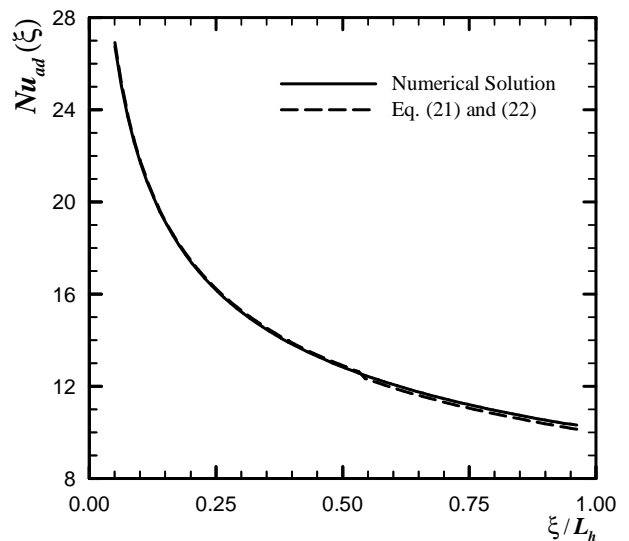


Figure 3. Comparison of the numerical results with predictions from Eqs. (21) and (22).

The influence coefficient g_h^* , defined by Eq. (17), was obtained from simulations for an adiabatic substrate wall, because this is the simplest procedure. For the adiabatic substrate, $\bar{T}_{ad} = T_{in}$ and all the heat is transferred directly to the airflow by convection, $q_f = q_h$. The results presented in Fig. 4 are, however, valid for either an adiabatic or a conductive substrate. They indicate that the coefficient g_h^* increases with the Reynolds number, due to larger mass flow rates. This coefficient was correlated to the Reynolds number by

$$g_h^* = 0.339 Re^{0.66} \tag{24}$$

The heater average adiabatic Nusselt number \bar{Nu}_{ad} , as defined by Eq. (12), was obtained considering an adiabatic substrate ($q_f = q_h$ and $q_u = 0$). The heater average adiabatic temperature was obtained from Eqs. (19) and (24) and the result was replaced on the right side of Eq. (12), giving rise to the correlation

$$\bar{Nu}_{ad} = 1.475 Pr Re^{0.34} \tag{25}$$

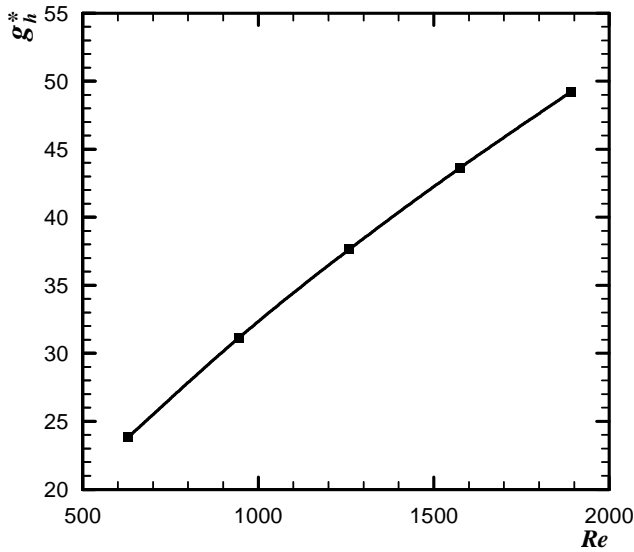


Figure 4. Heater influence coefficient g_h^*

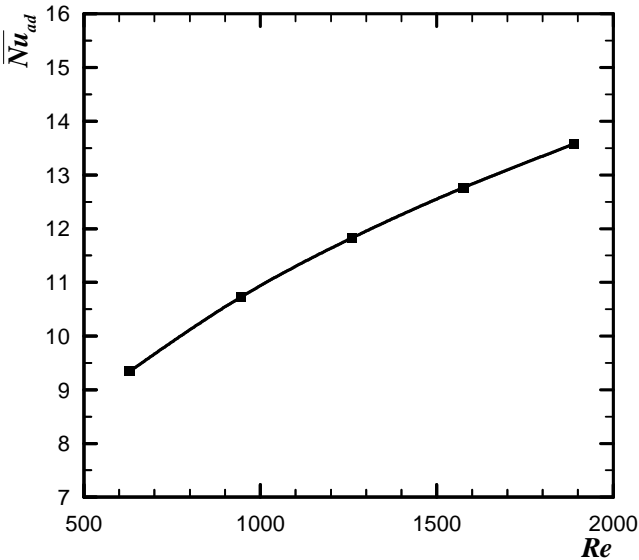


Figure 5. Heater average adiabatic Nusselt number for air.

This Nusselt number does not depend on the thermal conditions – it changes only with the flow conditions and the results for air ($Pr = 0.707$) are presented in Fig. 5 as a function of the Reynolds number.

For a conductive substrate, an upstream airflow heating q_u gives rise to a temperature increase ($\bar{T}_{ad} - T_{in}$). This temperature rise was expressed with the help of the upstream coefficient g_u^* defined by Eq. (16), obtained from the simulations of the conjugate problem. Considering for example $t/H = 0.5$, the dependence of the coefficient g_u^* on the Reynolds number is presented in Fig. 6, for distinct values of (k_s/k) . It increases with the Reynolds number, mainly due to larger mass flow rates. For a given Re , this coefficient decreases as (k_s/k) increases, due to larger upstream heating (q_u) through the substrate wall. The dependence on Re was similar for thinner substrates, but the values of g_u^* increased due to larger conductive spreading resistances associated with thinner walls.

Table 1 presents the numerical results of g_u^* for the ratio $(k_s/k) = 80$, encompassing the five substrate thicknesses and the five Reynolds numbers considered in the present work.

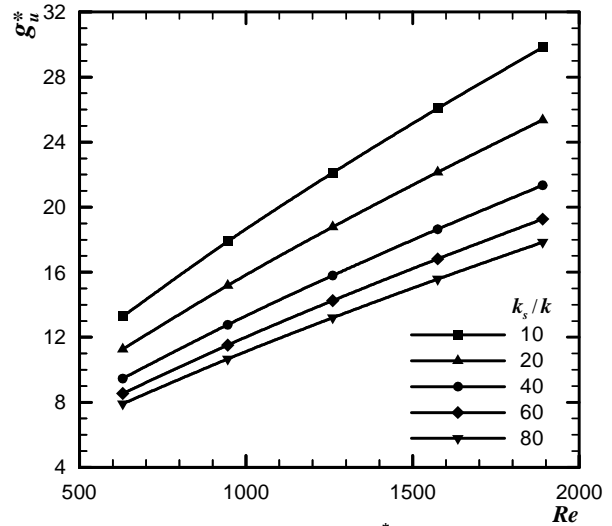


Figure 6. Upstream coefficient g_u^* for $t/H = 0.5$.

Table 1. Upstream coefficient g_u^* for $(k_s/k) = 80$.

t/H	Re				
	630	945	1260	1575	1890
0.1	11.7135	15.7673	19.4808	22.9660	26.2619
0.2	9.9132	13.3525	16.5058	19.4598	22.2690
0.3	8.9720	12.0842	14.9435	17.6347	20.1873
0.4	8.3516	11.2594	13.9273	16.4329	18.8213
0.5	7.9088	10.6621	13.1960	15.5729	17.8417

The heat transfer fractions (q_f/q_h), (q_s/q_h) and (q_u/q_h) were also obtained from the simulations of the conjugate problem. The first two fractions obviously add to unity, as can be checked by integration of Eq. (3) along the heater length, with the definitions of Eq. (10). The fraction (q_s/q_h) is presented in Fig. 7 for the substrate thickness $t/H = 0.5$, indicating that most of the heat transfer occurs through the substrate plate, except for the lowest (k_s/k) . As expected, the ratio (q_s/q_h) increased with the ratio (k_s/k) , due to smaller conductive spreading resistance, and it decreased as Re increased, due to larger direct convective heat transfer. The results of (q_s/q_h) for $(k_s/k) = 80$ are presented in Table 2, showing that for any Re it increases with the substrate thickness, due also to smaller conductive spreading resistance.

The fraction (q_u/q_h) conducted upstream of the heater for $t/H = 0.5$ is presented in Fig. 8, considering the effects of Re and the ratio (k_s/k) . The effect of the substrate thickness t on (q_u/q_h) is presented in Table 3 for $(k_s/k) = 80$. They follow a trend similar to (q_s/q_h) with respect to the effects of t , (k_s/k) and Re . Comparing the data in Table 2 and Table 3, it is seen that about 60 per cent of the conduction heat transfer from the heater to the substrate wall is released to the airflow upstream of the heater.

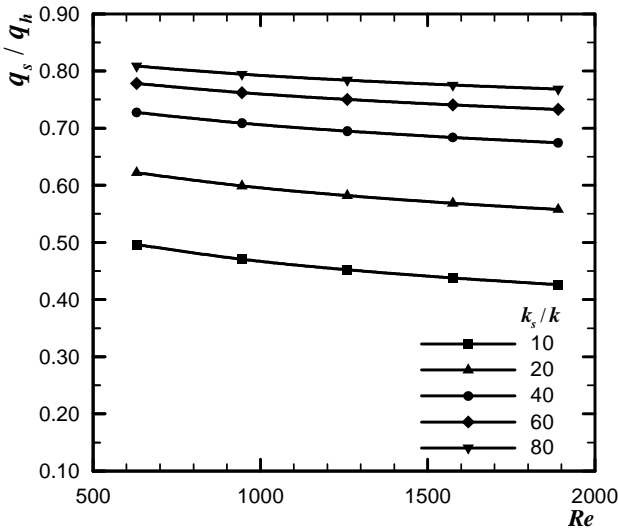


Figure 7. Fraction (q_s/q_h) for $t/H = 0.5$.

Table 2. Fraction (q_s/q_h) for $(k_s/k) = 80$.

t/H	Re				
	630	945	1260	1575	1890
0.1	0.6224	0.6012	0.5858	0.5737	0.5636
0.2	0.7170	0.6988	0.6854	0.6747	0.6658
0.3	0.7624	0.7460	0.7339	0.7243	0.7162
0.4	0.7899	0.7749	0.7637	0.7547	0.7472
0.5	0.8085	0.7944	0.7839	0.7754	0.7683

The heater average dimensionless temperature $\bar{\theta}_h$ was obtained from the previous results and the Peclet number (Pe), using Eq. (19). The distribution of $\bar{\theta}_h$ for $t/H = 0.5$ is presented in Fig. 9, showing the expected temperature decrease as the mass flow rates increases with the Reynolds number. It also shows the heater temperature decrease as the substrate thermal conductivity increases. The results for the thermal conductivities ratio $(k_s/k) = 80$ are presented in Table 4, showing that the heater average temperature decreases with the Reynolds number and the substrate thickness. The temperatures $\bar{\theta}_h$ presented in Table 4 were obtained from Eq. (19) and they matched those obtained directly from the numerical simulations within 10^{-4} .

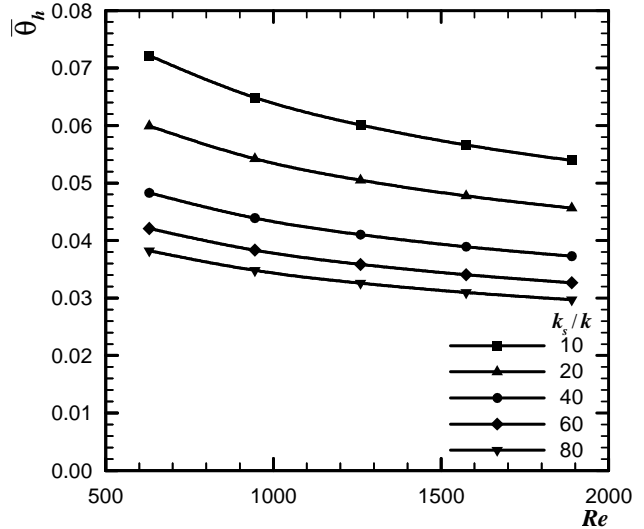


Figure 9. Dimensionless heater average temperature for $t/H = 0.5$.

Table 4. Dimensionless heater average temperature for $(k_s/k) = 80$.

t/H	Re				
	630	945	1260	1575	1890
0.1	0.0604	0.0545	0.0506	0.0478	0.0456
0.2	0.0499	0.0452	0.0421	0.0399	0.0382
0.3	0.0443	0.0403	0.0376	0.0357	0.0342
0.4	0.0408	0.0371	0.0347	0.0329	0.0316
0.5	0.0382	0.0348	0.0326	0.0310	0.0297

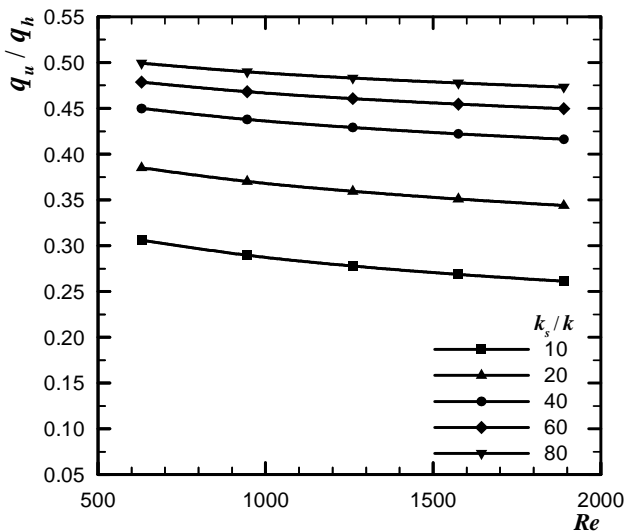


Figure 8. Fraction (q_u/q_h) for $t/H = 0.5$.

Table 3. Fraction (q_u/q_h) for $(k_s/k) = 80$.

t/H	Re				
	630	945	1260	1575	1890
0.1	0.3804	0.3665	0.3565	0.3487	0.3422
0.2	0.4401	0.4283	0.4196	0.4128	0.4072
0.3	0.4693	0.4587	0.4509	0.4448	0.4397
0.4	0.4873	0.4774	0.4702	0.4645	0.4597
0.5	0.4993	0.4899	0.4831	0.4777	0.4732

The heater average Nusselt number based on T_{in} depends on the ratio (k_s/k) and the Reynolds number. It may be obtained either directly from the numerical simulations, or from the previous results for (q_f/q_h) and $\bar{\theta}_h$, as indicated by Eq. (14). The \overline{Nu}_{in} distribution obtained for $t/H = 0.5$ is presented in Fig. 10. It increases with Re due to larger airflow rates, but decreases with (k_s/k) due to a larger conductance of the substrate wall. As the substrate thickness t decreases, larger conductive wall resistances increase \overline{Nu}_{in} , as indicated by the numerical results presented in Table 5 for the case with $(k_s/k) = 80$.

Compared to the adiabatic substrate, the conductive substrate provides additionally a conductive path for heat transfer from the heater. Considering the same inlet flow and heater average temperatures and flow rate in the channel, the conductive substrate causes an enhancement of heat transfer from the heater when compared to the adiabatic substrate. It was evaluated as follows. An adiabatic substrate transfers heat to the airflow only by convection, at a rate q_{ad} . For a conductive substrate, the direct convective heat

transfer from the heater to the airflow is equal to q_f . From the definitions of \overline{Nu}_{ad} and \overline{Nu}_{in} , Eq. (11) and (13), the ratio of these two heat transfer rates was expressed by

$$\frac{q_f}{q_{ad}} = \left(\frac{\overline{Nu}_{in}}{\overline{Nu}_{ad}} \right) \tag{26}$$

When the heat transfer rate q_f obtained from this equation is substituted into the heater overall energy balance, $q_h = (q_f + q_s)$, an expression for the heat transfer enhancement due to the conductive substrate is obtained in the form

$$\frac{q_h}{q_{ad}} = \left(\frac{\overline{Nu}_{in} / \overline{Nu}_{ad}}{1 - (q_s / q_h)} \right) \tag{27}$$

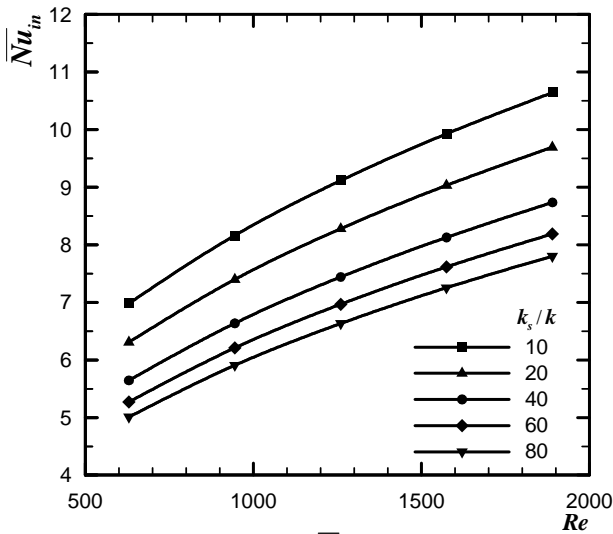


Figure 10. Heater \overline{Nu}_{in} for $t/H = 0.5$.

Table 5. Heater \overline{Nu}_{in} for $(k_s/k) = 80$.

t/H	Re				
	630	945	1260	1575	1890
0.1	6.2496	7.3200	8.1841	8.9206	9.5722
0.2	5.6738	6.6638	7.4642	8.1488	8.7523
0.3	5.3591	6.3070	7.0725	7.7246	8.3020
0.4	5.1548	6.0712	6.8140	7.4490	8.0081
0.5	5.0094	5.9070	6.6324	7.2541	7.8012

This result is presented in Fig. 11 for $t/H = 0.5$ and also in Table 6, for $(k_s/k) = 80$. The enhancement increases with both (k_s/k) and t , due to a greater conductance of the substrate wall. The effect of the Reynolds number is not obvious from Eq. (27) because, as can be seen from the previous results, the ratio $(\overline{Nu}_{in} / \overline{Nu}_{ad})$ increases with the Reynolds number, while the ratio (q_s/q_h) decreases, causing opposing trends to (q_h/q_{ad}) . In the present investigation, the effect of (q_s/q_h) was slightly dominant – the heat transfer enhancement decreased slightly with the Reynolds number. The presented results indicate a significant heat transfer enhancement due to substrate conduction – the heat transfer ratio (q_h/q_{ad}) ranged from about 150% to 280%.

Due to the substrate adiabatic lower surface, the heat conducted upstream of the heater through the substrate wall eventually returns to

the airflow and causes an increase $(\overline{T}_{ad} - T_{in})$ of the heater average adiabatic temperature above the inlet flow temperature. This undesirable temperature rise was compared to the total heater average temperature rise above the inlet flow temperature, $(\overline{T}_h - T_{in})$. From Eqs. (16) and (18):

$$\frac{\overline{T}_{ad} - T_{in}}{\overline{T}_h - T_{in}} = \frac{g_u^*}{\left(g_u^* + \frac{q_f}{q_u} g_h^* \right)} \tag{28}$$

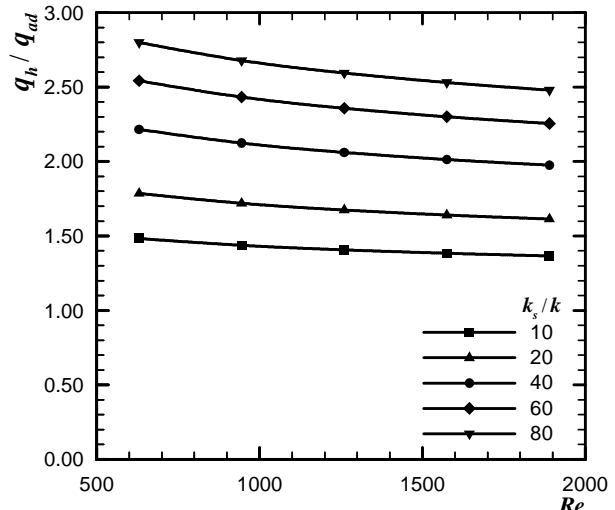


Figure 11. Heat transfer enhancement (q_h/q_{ad}) for $t/H = 0.5$.

Table 6. Heat transfer enhancement (q_h/q_{ad}) for $(k_s/k) = 80$.

t/H	Re				
	630	945	1260	1575	1890
0.1	1.7714	1.7113	1.6704	1.6397	1.6153
0.2	2.1457	2.0627	2.0058	1.9629	1.9286
0.3	2.4140	2.3151	2.2470	2.1955	2.1543
0.4	2.6259	2.5146	2.4378	2.3795	2.3329
0.5	2.7997	2.6786	2.5947	2.5309	2.4795

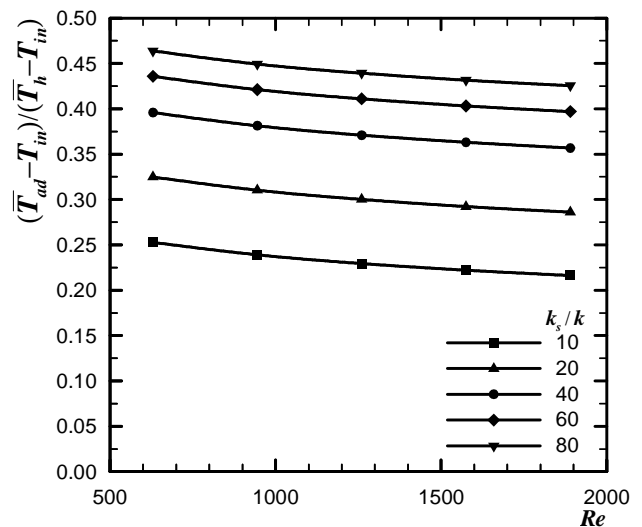


Figure 12. Ratio $(\overline{T}_{ad} - T_{in}) / (\overline{T}_h - T_{in})$ for $t/H = 0.5$.

Table 7. Ratio $(\overline{T}_{ad} - T_{in})/(\overline{T}_h - T_{in})$ for $(k_s/k) = 80$.

t/H	Re				
	630	945	1260	1575	1890
0.1	0.3311	0.3175	0.3081	0.3010	0.2951
0.2	0.3928	0.3787	0.3690	0.3615	0.3554
0.3	0.4264	0.4120	0.4021	0.3947	0.3886
0.4	0.4483	0.4340	0.4239	0.4163	0.4103
0.5	0.4639	0.4493	0.4393	0.4316	0.4255

The results obtained for the ratio of these temperature differences are presented in Fig. 12 for $t/H = 0.5$ and in Table 7 for $(k_s/k) = 80$, within the investigated range of the Reynolds number. They show that from 25% to 45% of the total heater average temperature rise is due to the thermal wake originating from the upstream heated floor of the conductive substrate. This ratio increases with the substrate conductivity and thickness, while it decreases slightly with the Reynolds number, as expected. It should be kept in mind, however, that the average adiabatic temperature rise is the effect of the enhanced total heat transfer from the heater. Under the same inlet flow conditions and heater average temperature, the direct convective heat transfer from the heater to the airflow is smaller for the conductive substrate than for the adiabatic substrate. This decrease is, however, more than compensated by the total heat transfer rate from the heater in the case of the conductive substrate, as it has been shown by the results presented in Fig. 11 and Table 6.

Conclusions

The conjugate forced convection and conduction heat transfer from a strip heater flush mounted to a finite thickness wall (substrate) of a parallel plates channel were investigated numerically, using the control volumes method. The investigation was performed considering laminar airflow fully developed from the channel entrance. A uniform heat flux q_h'' was released along the heater length and it was transferred to the airflow and to the conductive substrate wall. The local distribution into the direct convective heat flux $q_f''(x)$ from the heater to the airflow and the conductive heat flux $q_s''(x)$ from the heater to the substrate wall were not known a priori and they were obtained by an iterative procedure. These two heat fluxes were integrated along the heater length to evaluate its convective and conductive heat losses. The convective heat loss q_f was expressed by means of the adiabatic heat transfer coefficient, because it is independent of the thermal conditions. The heater average temperature $\overline{\theta}_h$ was expressed by means of two influence coefficients: the upstream influence coefficient g_u^* , and the self-heating influence coefficient g_h^* . The first coefficient evaluated the heater average adiabatic temperature rise above the inlet flow temperature in the channel, and the second coefficient was used to evaluate the average heater temperature rise above its average adiabatic temperature. Considering a dissipation rate q_h in the heater, the fraction (q_s/q_h) conducted through the substrate and the portion (q_u/q_h) conducted upstream of the heater were obtained numerically as functions of the channel Reynolds number, the thermal conductivities ratio (k_s/k) and the substrate thickness t . The results indicated that a substantial fraction of heat transfer occurs by conduction through the substrate. The average Nusselt numbers \overline{Nu}_{in} and \overline{Nu}_{ad} were related to evaluate the heat

transfer enhancement due to a conductive substrate in comparison to an adiabatic substrate, indicating values from 150% to 280%. The heater average adiabatic temperature rise due to preheating of the airflow by substrate conduction was related to its total temperature rise above T_{in} in dimensionless form, indicating that it represents a substantial fraction of the total, ranging from 25% to 45% in the present investigation.

Acknowledgements

The support of CNPq (Brazilian Research Council) to the first author in the form of a Doctorate Program Scholarship is gratefully acknowledged.

References

- Alves, T.A., 2010, "Conjugate Cooling of Discrete Heaters in Channels" (In Portuguese), Ph.D. Thesis, State University of Campinas, Campinas, SP, Brazil, 129 p.
- Alves, T.A. and Altemani, C.A.C., 2008, "Convective Cooling of Three Discrete Heat Sources in Channel Flow", *J. Braz. Soc. Mech. Sci. & Eng.*, Vol. XXX, pp. 245-252.
- Alves, T.A. and Altemani, C.A.C., 2010, "Thermal Design of a Protruding Heater in Laminar Channel Flow", Proceedings of the 14th International Heat Transfer Conference, Washington, USA, pp. 691-700.
- Anderson, A.M., 1994, "Decoupling Convective and Conductive Heat Transfer Using the Adiabatic Heat Transfer Coefficient", *ASME J. Electronic Packaging*, Vol. 116, pp. 310-316.
- Cole, K.D., 1997, "Conjugate Heat Transfer from a Small Heated Strip", *I. J. Heat Mass Transfer*, Vol. 40, pp. 2709-2719.
- Davalath, J. and Bayazitoglu, Y., 1987, "Forced Convection Cooling Across Rectangular Blocks", *ASME J. Heat Transfer*, Vol. 109, pp. 321-328.
- De Vahl Davis, G., 1983, "Natural Convection of Air in a Square Cavity: A Benchmark Numerical Solution", *I. J. Numerical Methods Fluids*, Vol. 3, pp. 249-264.
- Incropera, F.P., DeWitt, D.P., Bergman, T.L. and Lavine, A.S., 2006, "Fundamentals of Heat and Mass Transfer", John Wiley & Sons, Hoboken, USA, 1024 p.
- Incropera, F.P., Kerby, J.S., Moffat, D.F. and Ramadhyani, S., 1986, "Convection Heat Transfer from Discrete Heat Sources in a Rectangular Channel", *I. J. Heat Mass Transfer*, Vol. 29, pp. 1051-1057.
- Kang, B.H., Jaluria, Y. and Tewari, S.S., 1990, "Mixed Convection Transport from an Isolated Heat Source Module on a Horizontal Plate", *ASME J. Heat Transfer*, Vol. 112, pp. 653-661.
- Moffat, R.J., 1998, "What's New in Convective Heat Transfer?", *I. J. Heat Fluid Flow*, Vol. 19, pp. 90-101.
- Nakayama, W., 1997, "Forced Convective/Conductive Conjugate Heat Transfer in Microelectronic Equipment", *Annual Review Heat Transfer*, Vol. 8, pp. 1-45.
- Patankar, S.V., 1980, "Numerical Heat Transfer and Fluid Flow", Hemisphere Publishing Corporation, New York, USA, 197 p.
- Ramadhyani, S., Moffat, D.F. and Incropera, F.P., 1985, "Conjugate Heat Transfer from Small Isothermal Heat Sources Embedded in a Large Substrate", *I. J. Heat Mass Transfer*, Vol. 28, pp. 1945-1952.
- Shah, R.K. and London, A.L., 1978, "Laminar Flow Forced Convection in Ducts", *Advances in Heat Transfer*, Supplement No. 1, Academic Press, New York.
- Sugavanam, R., Ortega, A. and Choi, C.Y., 1995, "A Numerical Investigation of Conjugate Heat Transfer from a Flush Heat Source on a Conductive Board in Laminar Channel Flow", *I. J. Heat Mass Transfer*, Vol. 38, pp. 2969-2984.
- Wang, Q. and Jaluria, Y., 2004, "Three-Dimensional Conjugate Heat Transfer in a Horizontal Channel with Discrete Heating", *ASME J. Heat Transfer*, Vol. 126, pp. 642-647.
- Zeng, Y. and Vafai, K., 2009, "An Investigation of Convective Cooling of an Array of Channel-Mounted Obstacles", *Numerical Heat Transfer*, Part A, Vol. 55, pp. 967-982.